

# Influence of dynamic tissue properties on temperature elevation and lesions during HIFU scanning therapy: Numerical simulation\*

Xiao Zou(邹孝), Hu Dong(董胡), and Sheng-You Qian(钱盛友)<sup>†</sup>

School of Physics and Electronics, Hunan Normal University, Changsha 410081, China

(Received 20 December 2019; revised manuscript received 12 January 2020; accepted manuscript online 16 January 2020)

When large tumors are treated, ablation of the entire volume of tumors requires multiple treatment spots formed by high intensity-focused ultrasound (HIFU) scanning therapy. The heating effect of HIFU on biological tissue is mainly reflected in temperature elevation and tissue lesions. Tissue property parameters vary with temperature and, in turn, the distribution of temperature as well as the heating effects change accordingly. In this study, an HIFU scanning therapy model considering dynamic tissue properties is provided. The acoustic fields and temperature fields are solved combining the Helmholtz wave equation with Pennes bio-heat transfer equation based on the finite element method (FEM) to investigate the effects of various tissue properties (*i.e.*, the attenuation coefficient, acoustic velocity, thermal conductivity, specific heat capacity, density, and blood perfusion rate) on heating performance. Comparisons of the temperature distribution and thermal lesions under static and dynamic properties are made based on the data of tissue property parameters varying with temperature. The results show that the dynamic changes of thermal conductivity, specific heat capacity, and acoustic velocity may account for the decrease of temperature elevation in HIFU treatment, while the dynamic changes of attenuation coefficient, density, and blood perfusion rate aggravate the increase of temperature on treatment spots. Compared with other properties, the dynamic change of attenuation coefficient has a greater impact on tissue temperature elevation. During HIFU scanning therapy, the temperature elevation and tissue lesions of the first treatment spot are smaller than those of the subsequent treatment spots, but the temperature on the last treatment spot drops faster during the cooling period. The ellipsoidal tissue lesion is not symmetrical; specifically, the part facing toward the previous treatment spot tends to be larger. Under the condition of the same doses, the temperature elevation and the size of tissue lesions under dynamic properties present significant growth in comparison to static properties. Besides, the tissue lesion begins to form earlier with a more unsymmetrical shape and is connected to the tissue lesion around the previous treatment spot. As a result, lesions around all the treatment spots are connected with each other to form a closed lesion region. The findings in this study reveal the influence of dynamic tissue properties on temperature elevation and lesions during HIFU scanning therapy, providing useful support for the optimization of treatment programs to guarantee higher efficacy and safety.

**Keywords:** high intensity-focused ultrasound (HIFU), temperature elevation, tissue lesions, dynamic tissue properties

**PACS:** 43.35.+d, 43.80.+p

**DOI:** 10.1088/1674-1056/ab6c4f

## 1. Introduction

As a potential non-invasive method of tumor therapy, high intensity focused ultrasound (HIFU) shows great promise with excellent directivity, penetrability and focusing function, which has been used in clinical treatment for solid tumors, such as uterine fibroids and tumors in liver, breast, and prostate.<sup>[1–5]</sup> During HIFU therapy, ultrasound *in vitro* can be focused into the treatment region in the biological tissue, where the temperature could rise to above 65 °C within a short time after absorbing energy, so that the tumors would be induced to irreversible coagulation necrosis without damage to the surrounding tissue.<sup>[6–9]</sup>

Despite the uniqueness and remarkable clinical achievements of HIFU, there are still many important scientific problems unresolved, such as treatment program optimization and therapeutic effect evaluation during the treatment

process.<sup>[10,11]</sup> The heating effect of HIFU on biological tissue is mainly characterized with temperature elevation and tissue lesions, which can be used to adjust treatment programs. The acoustic intensity decreases exponentially as the ultrasound goes deeper into the tissue, and part of the energy would be absorbed by the tissue and converted to heat. The rate of heat change is related to the acoustic intensity and the absorption coefficient of the tissue, while the temperature elevation is subject to tissue absorption, thermal conduction, and blood perfusion. Absolute temperature of the tissue is the leading cause of thermal lesions, but the degree of tissue lesions is determined mostly by the accumulation of heat rather than by absolute temperature. The distribution of temperature elevation and equivalent thermal dose can better characterize the degree of coagulation necrosis in tissue.<sup>[12,13]</sup>

When tumors are large enough in diameter, ablation of the entire volume of tumors requires multiple treatment spots

\*Project partially supported by the National Natural Science Foundation of China (Grant Nos. 11774088 and 11474090), the Natural Science Foundation of Hunan Province, China (Grant Nos. 2016JJ3090 and 2018JJ3557), and the Scientific Research Fund of Hunan Provincial Education Department, China (Grant Nos. 16B155 and 17B025).

<sup>†</sup>Corresponding author. E-mail: shyqian@hunnu.edu.cn

administered over a treatment layer by either the ultrasound phased array with electronic scanning or the single source with mechanical scanning.<sup>[14]</sup> The ultrasound phased array has many advantages such as multi-focus, no mechanical movement, and short treatment time, but now it is rarely seen in commercial HIFU systems.<sup>[15]</sup> On the contrary, mechanical scanning is widely used in clinical therapy, in which the HIFU-sourced transducer or the biological tissue is moved at a certain step size to irradiate each treatment spot for a period of time to realize the superposition of individual treatment spots in terms of the treatment region, resulting in a large tissue lesion in size. However, during scanning therapy, the heating effect of the treatment point will be affected by neighboring treatment spots because of thermal diffusion and dynamic properties, and the consequent changes in temperature elevation and tissue lesions would make the treatment out of control.<sup>[16,17]</sup>

It had been proved that tissue property parameters change with temperature variation during HIFU therapy.<sup>[18,19]</sup> Clarke *et al.* found that the increase of attenuation coefficient under ultrasound was due to the irreversible changes in tissue structure, such as protein coagulation.<sup>[20]</sup> Zderic *et al.* validated that the ultrasonic coefficients of liver and spleen tissue after HIFU treatment were about twice as those before HIFU treatment from 1 MHz to 5 MHz.<sup>[21]</sup> Some studies have shown that when the temperature rises slowly, the blood vessels would expand and the blood flow velocity would increase to carry away more heat, and the blood perfusion rate would change with the temperature; once the tissue is denatured, the vascular system would collapse and close, and the blood perfusion rate would reduce to 0. The change of tissue properties caused by the heating of HIFU will in turn affect the heating effect of HIFU, including the redistribution of temperature field and the size of tissue lesions.<sup>[22–24]</sup> Sonesson compared the temperature distribution and the size of the therapeutic area formed under static and dynamic acoustic attenuation ignoring the influence of tissue nonlinearity.<sup>[25]</sup>

In this study, an HIFU scanning therapy model with dynamic tissue properties is proposed, and the acoustic fields and temperature fields are solved by finite element method (FEM) to study the influence of tissue properties (*i.e.*, the attenuation coefficient, acoustic velocity, thermal conductivity, specific heat capacity, density, and blood perfusion rate) on temperature elevation and lesions during scanning therapy. The associative influence of thermal diffusion and dynamic tissue properties on temperature distribution and tissue lesions are studied. The results reveal the influence of tissue properties on heating effect during HIFU scanning therapy, providing a reference for the optimization of treatment programs.

## 2. Theory and methods

An HIFU simulation model is established as shown in Fig. 1, where the ultrasonic transducer is located in the bot-

tom with a focal length of 16 cm and an aperture of 14 cm; there is a hole (diameter: 5 cm) on the center to facilitate the installation of a B-mode ultrasonic probe. The biological tissue, set as a cylinder 4 cm in radius and 6 cm in height, is placed directly above the ultrasonic transducer, and the focus of the ultrasonic transducer corresponds to the geometric center of the tissue. The ultrasonic transducer and tissue are both immersed in water. Acoustic absorbing rubber layer of 5 mm in thickness is set on the left, right, and upper of the model, so ultrasonic waves can be completely absorbed by the boundary to avoid reflections and scatterings. The drive transducer operates at a frequency of 1.391 MHz (all parameters of the transducer refer to PRO2008, Pro hitu, Shenzhen, China). The initial temperature of water and tissue in this model is assumed to be 37 °C, and properties parameters of tissue at this temperature are shown in Table 1.<sup>[26]</sup> During scanning therapy, the acoustic pressure near the inner surface of transducer is set to be constant at 0.8 MPa, which is far less than that of cavitation threshold (5.3 MPa).<sup>[27,28]</sup> The therapeutic dose remains the same for every treatment spot, and the heating process is completed at one time without interruption. After a treatment spot is heated, the transducer is moved by 4 mm to the next treatment spot along the radial direction of acoustic focus; each movement from one treatment spot to another for 4 mm takes 1 s, when the radiation from transducer is cancelled and heating stops.

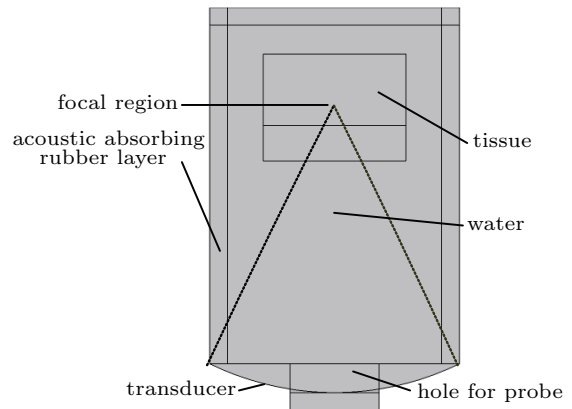


Fig. 1. Geometry of the HIFU model.

Assuming that the acoustic wave propagation is linear and the amplitudes of shear waves in the tissue domain are much smaller than those of the pressure waves, the nonlinear effects and shear waves are therefore neglected,<sup>[3]</sup> so the acoustic field can be described by a variable acoustic pressure and then solved by simulation using the approximate Helmholtz wave equation in two-dimensional coordinates as follows:<sup>[26,29]</sup>

$$\nabla \cdot \left( \frac{-1}{\rho_c} (\nabla p - q_d) \right) - \frac{((\omega/c_c)^2 - K_z^2) p}{\rho_c} = Q_d. \quad (1)$$

Table 1. Properties parameters of tissue at 37 °C.

Material	Density (/kg/m <sup>3</sup> )	Acoustic velocity/(m/s)	Attenuation coefficient/(Np/m)	Specific heat capacity/(J/(kg·K))	Thermal Conductivity/(W/(m·K))	Blood perfusion rate/(kg/(m <sup>3</sup> ·s))
Water	1000	1483	0.025	N/A	N/A	N/A
Tissue	1036	1551	3.5614	3560	0.5212	3.6

Here,  $p$  is acoustic pressure,  $\omega$  is the angular frequency,  $\nabla p$  is acoustic pressure derivative of space,  $K_z$  is out-of-plane wave number, while  $Q_d$  and  $q_d$  are possible unipolar and dipolar source, respectively;  $K_z$ ,  $Q_d$ , and  $q_d$  are set to be equal to 0 in this study. The density  $\rho_c$  and acoustic velocity  $c_c$  are complex-valued to account for properties of medium.

When the plane ultrasonic wave is propagating in the medium, if the acoustic field and intensity field are given, the heat can be calculated by

$$Q = 2 \cdot \alpha \cdot I = \alpha \cdot \frac{|p|^2}{\rho c}, \quad (2)$$

where  $\alpha$  stands for the absorption coefficient, equals to the attenuation coefficient in this study;  $I$  is the acoustic intensity magnitude, and  $Q$  is the absorbed ultrasound energy.<sup>[30,31]</sup>

The temperature elevation in tissue caused by the transformation of acoustic energy into heat can be calculated by Pennes bio-heat transfer equation (BHTE) written as<sup>[32]</sup>

$$\rho C \frac{\partial T}{\partial t} = \nabla \cdot (k \nabla T) + W_b C_b (T_a - T) + Q_p + Q_m. \quad (3)$$

In Eq. (3),  $\rho$  is the density of tissue,  $C$  and  $C_b$  are specific heat capacities of tissue and blood,  $T$  and  $T_a$  are temperatures of tissue and arterial blood, respectively;  $k$  is thermal conductivity

of tissue,  $W_b$  is blood perfusion rate,  $Q_p$  is heat-absorbed energy, and  $Q_m$  is metabolic rate. In fact, the time interval among treatments and the formation of tissue lesion is so short that we can ignore the metabolic heat and regard the heat source power  $Q_p$  as a complete result of the heat change by ultrasound radiation in Eq. (2).

According to the Arrhenius equation, the damage rate  $d\Omega/dt$  can be described as follows:<sup>[33]</sup>

$$\frac{d\Omega}{dt} = A \cdot \exp \left[ \frac{-E}{RT(t)} \right]. \quad (4)$$

Here,  $A$  is frequency factor, indicating the number of molecular collisions when tissue is heated to damage.  $E$  is activation energy,  $R$  is universal gas constant, and  $T(t)$  is absolute temperature of the tissue. Assuming that the biological tissue is divided into two parts, one part has been denatured while the other part is not. Then, the thermal damage degree ( $\Omega$ ) of the tissue at  $t$  obtained by integrating the damage rate with the time of heating, can be calculated by the follow equation:

$$\Omega = A \int_{t_0}^t \exp \left[ \frac{-E}{RT(\tau)} \right] d\tau, \quad (5)$$

where the thermal damage will be irreversible in the tissue when  $\Omega$  equals 1.

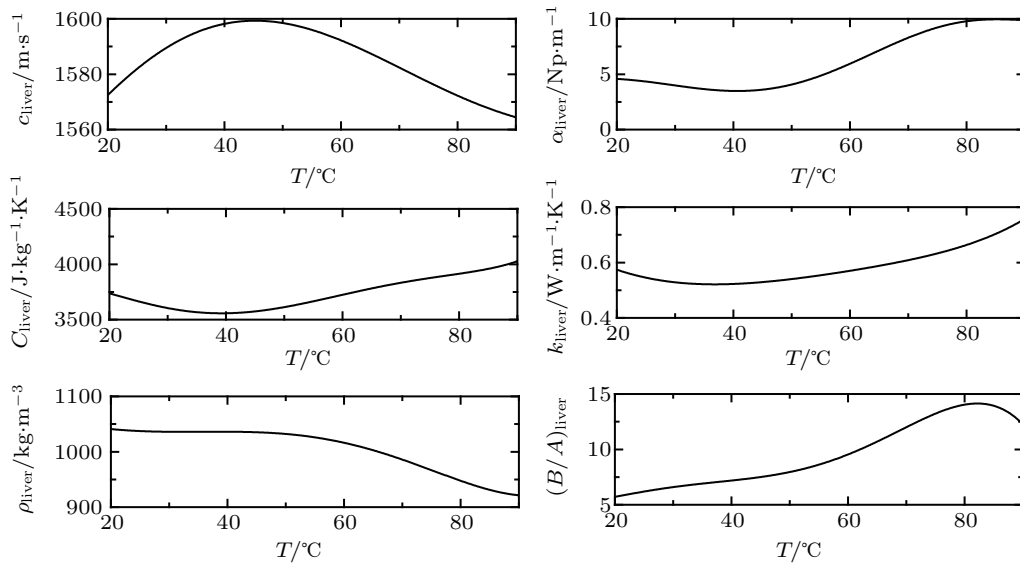


Fig. 2. Variations of liver tissue properties with temperatures.

In this study, if there are no tissue lesions, the blood perfusion rate can be seen unchanged, otherwise the blood perfusion rate should be defined to be 0. As is shown in

Fig. 2, tissue property parameters with temperature are derived from measurements by Damianou, Bamber, Choi, Gunter, *et al.*,<sup>[18,22,23,34]</sup> and the expression of property with temperature

in tissue is obtained from Fig. 2 through the polynomial approximation method according to the least square theory.<sup>[35]</sup> The calculation of temperature and lesions in tissue by finite element method (FEM) can be considered as a nonlinear solving process.<sup>[36]</sup> The initial value of acoustic and thermal parameters is shown in Table 1, and the time step length, marked as  $\Delta t$ , is set to be 0.2 s. The spatial grids for the simulation are 0.5 mm. After the distribution of ultrasonic pressure is

calculated by Eq. (1) given acoustic parameters, the heat absorbed, obtained based on acoustic attenuation coefficient by Eq. (2), is used to calculate the temperature fields by Eq. (3) combining thermal parameters, and then the temperature can be applied to evaluate tissue lesions by Eq. (5) and generate new acoustic and thermal parameters for next time node calculation according to Fig. 2. The calculation process is shown schematically in Fig. 3.

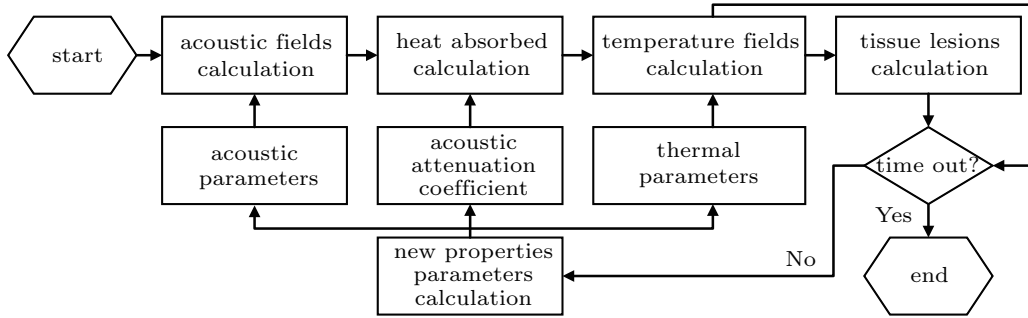


Fig. 3. Schematic diagram of the computation by FEM.

### 3. Results and discussion

#### 3.1. Influence of dynamic tissue properties on temperature elevation

The tissue *in vitro* is selected and kept under continuous and uninterrupted irradiation for 8 s. Considering the variations of tissue properties with temperature, comparisons of temperature elevation under static and dynamic properties with the same doses on single treatment spot are made as shown in Fig. 4, where the tissue is heated from 0 s to 8 s and cooled from 8 s to 16 s. During the heating process, the temperature is rising continuously and reaches its maximum at 8 s simultaneously. In comparison, the temperature drops very slowly during the cooling process. It can be found that all of the tissue temperature elevation curves are roughly coincident during the first two seconds of heating. During the latter 8 s, the rate of temperature change under dynamic attenuation coefficient would increase sharply, while the temperature elevation under other dynamic properties only shows slight differences from that under static properties, and the temperature elevation curves gradually seem to overlap the curve under static properties.

Table 2 shows the differences of temperature elevation on single treatment spot under dynamic and static properties parameters. It can be seen that the thermal conductivity, heat capacity, and acoustic velocity have negative effects on temperature elevation, while the density, blood perfusion rate, and attenuation coefficient are positively correlated to temperature elevation. Particularly, the attenuation coefficient, in comparison to other properties parameters, plays a leading role in influencing temperature elevation.

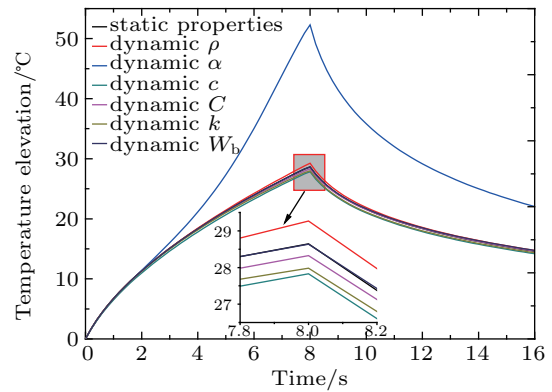


Fig. 4. Influence of dynamic tissue properties on temperature elevation.

Table 2. Temperature elevation deviation from under static properties at 8 s.

Tissue properties	Temperature elevation deviation on focus/°C
Thermal conductivity ( $k$ )	-0.67
Specific heat capacity ( $C$ )	-0.33
Density ( $\rho$ )	0.62
Acoustic velocity ( $c$ )	-0.82
Attenuation coefficient ( $\alpha$ )	23.64
Blood perfusion rate ( $W_b$ )	0.02

#### 3.2. Temperature elevation for various scanning spots

The formation of four treatment spots caused by three movements to the right along the radial direction of acoustic focus during HIFU scanning therapy is to be studied in this paper. Each treatment spot is set to be heated continuously for 8 s, and there would be a cooling period for 16 s after the last treatment spot is heated. The comparison of temperature elevation with time on four treatment spots between

static and dynamic properties is shown in Fig. 5, where the temperature elevation on all four treatment spots reaches the maximum at the completion of heating. The latter three spots share similar maximum values in terms of temperature elevation, which are higher than that on the first treatment spot. During the cooling period, the temperature trends of the first two treatment spots keep in agreement, and the temperature on the latter treatment spot is higher than that on the previous spot at the same moment. The temperature on the last treatment spot decreases rapidly, crossing with the curve of the third treatment spot at 48.2 s. During the time the previous spot is heated and the transducer is moving, the temperature on the latter treatment spot would have a slight elevation. In Fig. 5(a), the temperature–time curve of the first treatment spot is completely consistent with that under static properties discussed above in Fig. 4, reaching the same maximum value (28.5 °C) at 8 s. In comparison, the temperature elevation on the subsequent three focuses are 30.85 °C, 30.93 °C, and 30.93 °C respectively, which are at least 2.35 °C higher than that on the first focus. In Fig. 5(b), the maximum value on the first treatment spot is up to 42.64 °C, approximating the temperature elevation at 8 s under dynamic attenuation coefficient (42.29 °C) in Fig. 4. The maximum values on the latter

three treatment spots are above 48.75 °C, which are at least 6.11 °C higher than that on the first treatment spot. Comparing Fig. 5(a) with Fig. 5(b), because of the influence of dynamic properties, the temperature elevation under dynamic properties presents significant growth in comparison to static properties, and the temperature elevation deviation between the first and the subsequent three focuses is enlarged. Meanwhile, the trend of temperature elevation curve in Fig. 5(b) is similar to that under dynamic attenuation coefficient in Fig. 4, that can also verify that the dynamic change of attenuation coefficient has a greater impact on temperature elevation.

### 3.3. Lesions formation in tissue during HIFU scanning therapy

The tissue lesions under static and dynamic properties using the same doses are shown in Fig. 6 and Fig. 7, respectively, where panels (a), (b), (c), and (d) present lesions when each treatment spot has just been heated (at 8 s, 17 s, 26 s, 35 s), while panels (e) and (f) show lesions when the last treatment spot is cooled for 8 s and 16 s right after heated. In Fig. 6, there is no lesions formation at 8 s, and the lesion around the first treatment spot begins to appear during the heating of the second treatment spot (8 s–17 s). For the subsequent three treatment spots, their lesions are forming during their own heating process, but they are small in size. The lesions around all treatment spots are basically in the shape of an ellipse, which gradually increase in size after being heated for a period of time. The tissue lesions around the second and third treatment spot are roughly consistent in size at 51 s, much larger than that around the first treatment spot. Besides, the tissue lesion around each treatment spot is isolated from each other, presenting no denaturalization between two adjacent treatment spots. In Fig. 7, all lesions occur when the current treatment spot is heated and gradually expand over a period of time after the heating. At the moment when the current treatment spot is heated, the lesions around the four treatment spots present regular ellipses; lesions around the subsequent three treatment spots are basically equal in size, which are significantly larger than the first one. However, after a period of cooling time, the difference between the size of the first and the latter three lesions is expanding. Moreover, the lesions in ellipsoid shapes exhibit asymmetry, which are expanding toward the tissue lesions of the previous treatment spot. Consequently, all the treatment spots are connected with another and form a closed lesion region under dynamic properties, which would be more likely to happen with the help of some methods including increasing acoustic intensity, prolonging heating time and reducing movement distance.

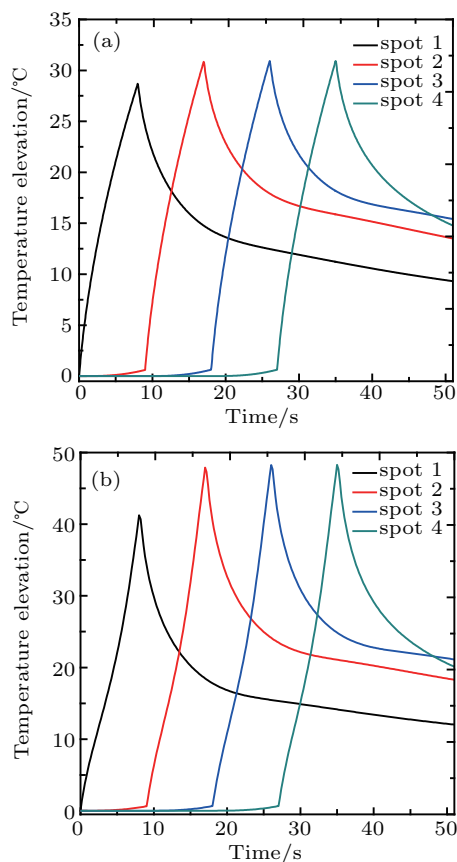


Fig. 5. Temperature elevation on four treatment spots during HIFU scanning therapy: (a) static properties; (b) dynamic properties.

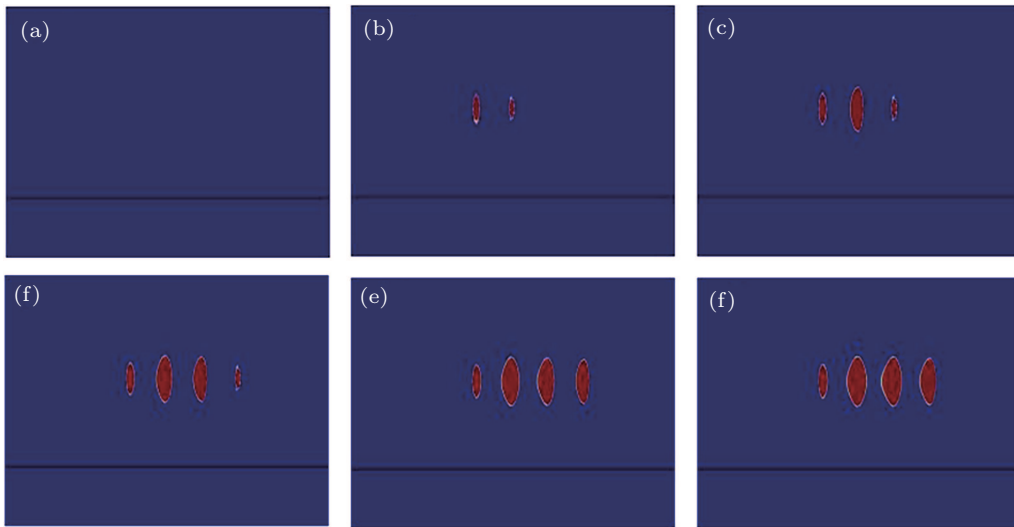


Fig. 6. Tissue lesions at different time under static properties: (a) 8 s; (b) 17 s; (c) 26 s; (d) 35 s; (e) 43 s; (f) 51 s.

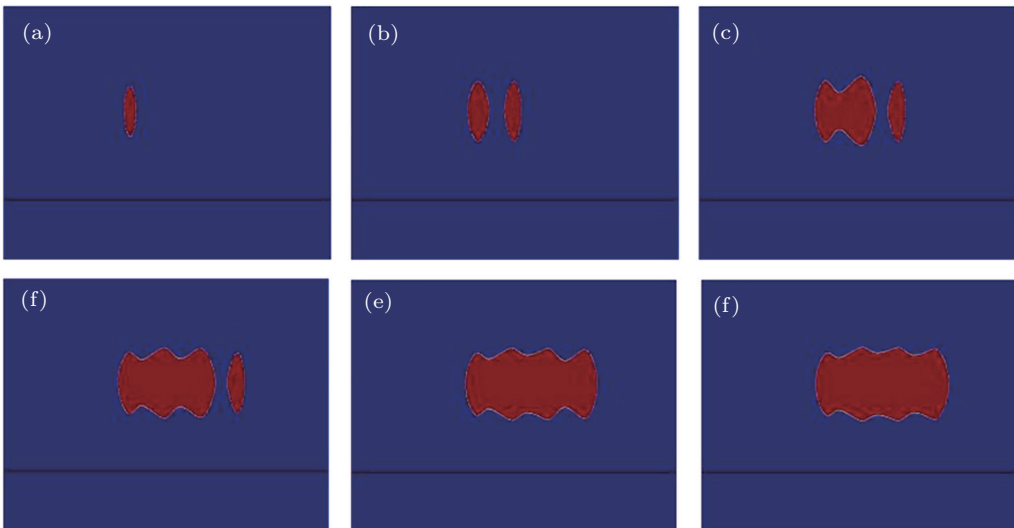
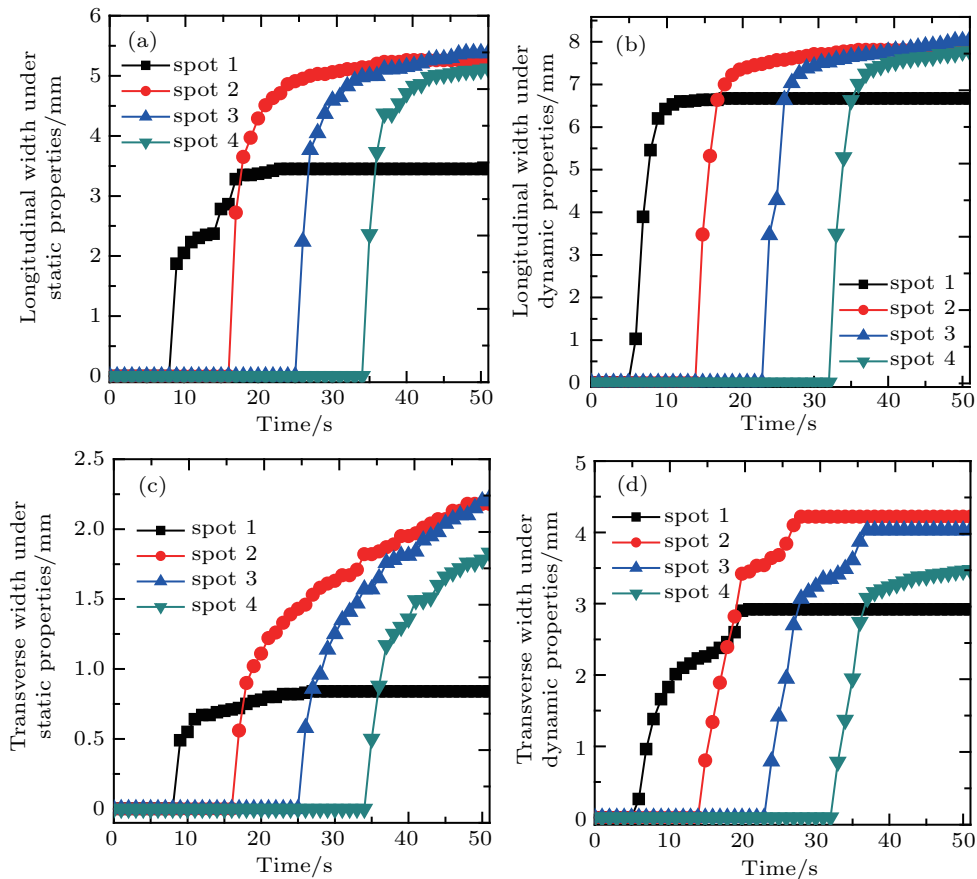


Fig. 7. Tissue lesions at different time under dynamic properties: (a) 8 s; (b) 17 s; (c) 26 s; (d) 35 s; (e) 43 s; (f) 51 s.

### 3.4. Changes of lesion sizes with time

The longitudinal and transverse widths of the tissue lesions under static and dynamic properties are illustrated in Fig. 8. The lesions around each treatment spot begin to appear at 9 s, 17 s, 26 s, and 35 s, respectively under static properties, and 6 s, 15 s, 24 s, and 33 s under dynamic properties, respectively. Obviously, the appearance of lesion around the first treatment spot under dynamic properties is 3 s earlier than that under static properties. For the subsequent three treatment spots, the occurrences of lesions under dynamic properties are 2 s earlier than those under static properties. Once lesions appear, the longitudinal and transverse width increase rapidly within a few seconds and then begin to level off. According to the comparison of Fig. 8(a) with Fig. 8(b), it costs the four lesions 9 s, 8 s, 7 s, and 6 s respectively for their longitudinal widths to grow steady under static properties, while the amount of time under dynamic properties would be only 5 s, 4 s, 4 s, and 4 s, respectively. Compared with those under

static properties, the lesions under dynamic properties increase at a faster rate in size and present smoother longitudinal width curves. In Fig. 8(c), during the cooling period, the transverse width of lesion around the first treatment spot changes slowly, which fixes to 0.84 mm after 27 s. In contrast, the transverse widths of lesions around the subsequent three treatment spots are increasing all the time until they reach 2.18 mm, 2.22 mm, and 1.83 mm at 51 s, respectively. In Fig. 8(d), the transverse widths of lesions around the first three treatment spots have no changes after growing to 2.92 mm, 4.22 mm, and 4.03 mm, respectively, but for the last treatment spot, the transverse width rises sharply and then grows slowly. During the scanning therapy, apart from the heat source of current treatment spot, lesion width is also affected by thermal diffusion and changes of tissue properties from neighboring treatment spots, which have a greater impact on lesion size along the transverse axis direction.



**Fig. 8.** Variations of lesion widths with time for four treatment spots, (a) and (b) longitudinal width under static properties and dynamic properties respectively; (c) and (d) transverse width under static properties and dynamic properties respectively.

#### 4. Conclusions

The heating effect of HIFU on biological tissue is subject to tissue properties. Compared with static tissue properties, the heating effect under dynamic properties presents higher temperature elevation and causes greater tissue lesions. The dynamic change of attenuation coefficient, in comparison of other parameters, has a greater impact on tissue temperature elevation, playing a critical role in influencing temperature elevation among all the tissue properties. During scanning therapy, the temperature elevation on the first treatment spot are much smaller than that on other treatment spots, but the temperature on the last treatment spot drops faster during the cooling period. Besides, the temperature elevation under dynamic properties presents significant growth in comparison to static properties. The shape of ellipsoidal tissue lesion is not symmetrical and the part facing toward the previous treatment spot tends to be larger. Compared with those under static properties, the tissue lesions under dynamic properties, generate with a more unsymmetrical shape and is connected to the tissue lesion around the previous treatment spot. Consequently, all the lesions around four treatment spots are connected with each other to form a closed lesion region. Furthermore, the lesions increase rapidly in size within a few seconds and then begin to level off, but the lesions under dynamic properties begin to appear earlier with larger size, and increase at a faster

rate in width. In HIFU clinical therapy, because of the influence of dynamic properties and thermal diffusion, a closed region connected with multiple large lesions is likely to happen, which is also affected by acoustic intensity, movement distance, and heating time, but excessive large size lesions would bring about over treatment and damage to surrounding tissue. On the other hand, differences of temperature elevation and lesion of each treatment spot may cause insufficient treatment around some treatment spots and over treatment around other treatment spots. Therefore, modification and optimization of HIFU treatment programs is necessary to form appropriate uniform lesions, which will guarantee higher efficacy and safety. In this paper, the scanning path is limited to two-dimensional because of the complexity of modeling and calculation, but the results obtained here have guiding significance for clinical application of HIFU.

#### References

- [1] Chang S H, Cao R, Zhang Y B, Wang P G, Wu S J, Qian Y H and Jian X Q 2018 *Chin. Phys. B* **27** 078701
- [2] Wang H L, Fan P F, Guo X S, Tu J, Ma Y and Zhang D 2016 *Chin. Phys. B* **25** 124314
- [3] Wang X D, Lin W J, Su C and Wang X M 2018 *Chin. Phys. B* **27** 024302
- [4] Kennedy J E, ter Haar G R and Cranston D 2003 *Br. J. Radiol.* **76** 590
- [5] Clement G T 2004 *Ultrasonics* **42** 1087

- [6] Illing R O, Kennedy J E, Wu F, ter Haar G R, Protheroe A S, Friend P J, Gleeson F V, Cranston D W, Phillips R R and Middleton M R 2005 *Br. J. Cancer* **93** 890
- [7] Hsiao Y H, Kuo S J, Tsai H D, Chou M C and Yeh G P 2016 *J. Cancer* **7** 225
- [8] Kovatcheva R, Vlahov J, Stoinov J, Lacoste F, Ortune C and Zaletel K 2014 *Eur. Radiol.* **24** 2052
- [9] Fruehauf J H, Back W, Eiermann A, Lang M C, Pessel M, Marlinghaus E, Melchert F, Volz-Köster S and Volz J 2008 *Arch. Gynecol. Obstet.* **277** 143
- [10] Murat F J L and Gelet A 2008 *Curr. Urol. Rep.* **9** 113
- [11] Zhou Y F 2011 *World. J. Clin. Oncol.* **2** 8
- [12] Nyborg W L, Hill C R and Bamber J C 2004 *J. Acoust. Soc. Am.* **117** 15
- [13] Damianou C and Hynynen K 1993 *Ultrasound Med. Biol.* **19** 777
- [14] Malinen M, Huttunen T, Kaipio J P and Hynynen K 2005 *Phys. Med. Biol.* **50** 3473
- [15] Zhou Y, Kargl S G and Hwang J H 2011 *Ultrasound Med. Biol.* **37** 1457
- [16] Fan X and Hynynen K 1996 *Ultrasound Med. Biol.* **22** 471
- [17] Curiel L, Chavier F, Gignoux B, Pichardo S, Chesnais S and Chapelon J Y 2004 *Med. Biol. Eng. Comput.* **42** 44
- [18] Damianou C A, Sanghvi N T, Fry F J and Maass-Moreno R 1997 *J. Acoust. Soc. Am.* **102** 628
- [19] Patel U H, Babbs C F, Deford J A, Bleyer M W, Marchosky J A and Moran C J 1992 *Med. Biol. Eng. Comput.* **30** 651
- [20] Clarke R L, Bush N L and ter Haar G R 2003 *Ultrasound Med. Biol.* **29** 127
- [21] Zderic V, Keshavarzi A, Vaezy S and Martin R W 2004 *Ultrasound Med. Biol.* **30** 61
- [22] Bamber J C and Hill C R 1979 *Ultrasound Med. Biol.* **5** 149
- [23] Choi M J, Guntur S R, Lee J M, Paeng D G and Lee K I L 2011 *Ultrasound Med. Biol.* **37** 2000
- [24] Liu D, Xu Z Y, Xia R M, Shou W D and Qian D C 2007 *Technic. Acoust.* **26** 62 (in Chinese)
- [25] Sonesson J E 2010 *The 9th International Symposium on Therapeutic Ultrasound*, September 24–26, 2009, Aix-en-Provence, France, p. 164
- [26] Su H D, Guo G P, Ma Q Y, Tu J and Zhang D 2017 *Chin. Phys. B* **26** 054302
- [27] Kullervo H 1991 *Ultrasound. Med. Biol.* **17** 157
- [28] Haddadi S Ahmadian M T 2018 *J. Ultras. Med.* **37** 1481
- [29] Guo G P, Su H D, Ding H and Ma Q Y 2017 *Acta Phys. Sin.* **66** 164301 (in Chinese)
- [30] Palmeri M L, Sharma A C, Bouchard R R, Nightingale R W and Nightingale K R 2005 *IEEE Trans. Ultrason. Ferroelectr. Freq. Control* **52** 1699
- [31] Hou G Y, Marquet F, Wang S and Konofagou E E 2014 *Phys. Med. Biol.* **59** 1121
- [32] Pennes H H 1948 *J. Appl. Physiol.* **1** 93
- [33] Galwey A K and Brown M E 2002 *Thermochim. Acta* **386** 91
- [34] Guntur S R, Lee K I, Paeng D G, Coleman A J and Choi M J 2013 *Ultrasound Med. Biol.* **39** 1771
- [35] Tan Q L, Zou X, Ding Y J and Zhao X M 2018 *Appl. Sci.* **8** 1993
- [36] Guntur S R and Choi M J 2015 *Ultrasound Med. Biol.* **41** 806